Synthesis, Crystal Structure and Quantum Chemistry of a Pb(II) Coordination Polymer Based on Adipic Acid and Phenanthroline Derivatives①

PAN Ya-Ru[a] LI Xiu-Mei[a②] LIU Bo[b②] ZHOU Shi[b]

[a] (*Faculty of Chemistry, Tonghua Normal University, Tonghua* 134002, *China*)

[b] (*Faculty of Chemistry, Jilin Normal University, Siping* 136000, *China*)

ABSTRACT A new Pb(II) coordination polymer, $[Pb(adip)(L)_2]_n$ (**1**, H_2adip = adipic acid, L = 2-(4-N,N′-dimethylphenyl)-1-H-imidazo[4,5-*f*][1,10]phenanthroline), was synthesized under hydrothermal conditions and characterized by single-crystal X-ray diffraction, powder XRD, FT-IR, thermogravimetric, fluorescence spectrum and elemental analysis techniques. Complex **1** crystallizes in triclinic system, space group $P\bar{1}$ with a = 11.406(3), b = 12.036(4), c = 17.520(5) Å, V = 2228.3(11) Å^3, M_r = 1028.09, D_c = 1.532 g·cm^{-3}, F(000) = 1024, μ(Mo$K\alpha$) = 3.842, R_{int} = 0.0274 and Z = 2. The final R = 0.1055 and wR = 0.3277 for 6954 observed reflections with $I > 2\sigma(I)$. It features a one-dimensional chain linked by adip^{2-} ligand. Moreover, complex **1** exhibits strong green luminescence with emission peak of 514 nm. In addition, the quantum-chemical calculations were accomplished on ′molecular fragments′ extracted from the crystal structure of **1** using the PBE0/LANL2DZ method built in Gaussian 16 Program. The calculation values denoted the distinct covalent interaction between the coordinated atoms and Pb(II) ion.

Keywords: coordination polymer, hydrothermal synthesis, crystal structure, luminescence property, quantum-chemical; DOI: 10.14102/j.cnki.0254-5861.2011-3195

1 INTRODUCTION

Lead(II) coordination polymers (CPs) are an active research topic in functional materials and have received much attention, not only because of their unique structural tailoring abilities and compositional diversity but also of their appealing applications in adsorption separation and luminescence[1-5]. The variety of their structures and properties relies on their multitudinous components and diverse assembly methods; these are directly related to the coordination characteristics of the components, such as organic ligands, solvent systems, temperature, charge, number of dentates, positions and types of substituents, and steric hindrance of the ligands[6, 7]. Although many CPs with intriguing topologies have been reported, the control of precise structures of CPs remains a great challenge in the crystal engineering field[8, 9].

The strategy of mixed ligands can indeed afford excellent new CPs with promising properties[10, 11]. However, the resulting structures are somewhat unpredictable, and their directed synthesis is still a challenge[12, 13]. Organic carboxylates are remarkable building blocks in the construction of CPs; they are considered to be good mixed ligand components because of their ability to balance charges, their good coordination ability and their stability in acid and base conditions[14-16]. On the other hand, phenanthroline derivatives are regarded as excellent organic building blocks[17, 18]. First, they not only have various types but also show excellent coordination ability in the process of assembly with metal ions. Secondly, they have variable conformations and good supporting capacity because of their rigid organic skeletons. Thus, it is meaningful to investigate the effects of the combination of carboxylates and phenanthroline derivative ligands on tuning the architectures of CPs.

Based on the above considerations, flexible adipic acid and rigid 2-(4-N,N′-dimethylphenyl)-1-H-imidazo[4,5-*f*][1,10] phenanthroline mixed ligands were selected to react with Pb(II) cations. As a result, a new one-dimensional complex of $[Pb(adip)(L)_2]_n$ (**1**) was obtained under hydrothermal condi-

Received 26 March 2021; accepted 13 May 2021 (**CCDC 2073304**)

① The project was supported by Jilin Science and Technology Development Program (JJKH20180776KJ) and Jilin Normal University Graduate Innovation Program (201939)

② Corresponding authors. Li Xiu-Mei, E-mail: lixm20032006@163.com; Liu Bo, E-mail: 112363305@qq.com

tions and structurally characterized by single-crystal X-ray diffraction, powder XRD, FT-IR, fluorescence spectrum, elemental analysis techniques and quantumchemical calculations. Complex **1** exhibits green photolu-minescence with an emission maximum at ca. 514 nm upon excitation at 320 nm. Quantum chemical calculations indicate significant covalent interaction between the coordination atoms and Pb(II) ion.

2 EXPERIMENTAL

2. 1 Materials and methods

2-(4-N,N′-dimethylphenyl)-1-H-imidazo[4,5-*f*][1,10] phenanthroline (L) was prepared according to a reported method[19]. All the other chemicals purchased were of reagent grade and used without further purification. IR spectra (KBr pellets) and powder X-ray diffraction were performed with a Varian-640 spectrometer and an Ultima IV diffractometer (40 kV and 40 mA, Cu$K\alpha$), respectively. The luminescence spectra and elemental analyses for C, N and H were obtained with a Hitachi F-7000 fluorescence/phosphorescence spectrometer and a PE 2400C elemental analyzer, respectively.

2. 2 Preparation of the complex

A mixture of $Pb(NO_3)_2$ (0.2 mmol, 0.0662 g), H_2adip (0.20 mmol, 0.0292 g), L (0.20 mmol, 0.0676 g), NaOH (0.4 mmol, 0.016 g), and H_2O (8 mL) was sealed in a 25 mL Teflon-lined autoclave under autogenous pressure at 120 ℃ for 5 days. After cooling to room temperature at a rate of 5 ℃ per hour, reddish-brown block crystals of **1** suitable for X-ray diffraction were obtained in 24.0% yield based on Pb(II). Anal. Calcd. (%) for $C_{48}H_{40}N_{10}O_4Pb$: C, 56.08; H, 3.92; N 13.62. Found (%): C, 55.88; H, 3.08; N, 13.03. IR (KBr, cm^{-1}): 3445(w), 3150(w), 1602(s), 1587(m), 1558(w), 1526(w), 1471(w), 1451(w), 1403(m), 1315(w), 1295(s), 1197(w), 1165(w), 1126(m), 1024(w), 856(w), 829(w), 810(w), 755(w), 735(w), 703(w), 686(w), 640(w), 519(w), 465(w).

2. 3 Determination of the crystal structures

The X-ray intensity data for **1** were collected on a Bruker D8 QUEST CMOS diffractometer, and the related crystal structure was solved by direct methods using the SHELXS and SHELXL programs of the SHELXTL crystallographic software package and refined on F^2 by the full-matrix least-squares method[20, 21]. The non-hydrogen atoms were refined with anisotropic temperature parameters and the hydrogen atoms of organic ligands were placed in calculated positions and treated as riding atoms with isotropic displacement parameters set at 1.2 to 1.5 times the U_{eq} values of the parent atoms. Selected bond lengths and bond angles are listed in Table 1.

Table 1. Selected Bond Lengths (Å) and Bond Angles (°) for 1

Bond	Dist.	Bond	Dist.	Bond	Dist.
Pb(1)–O(1)	2.448(14)	Pb(1)–O(3)	2.535(17)	Pb(1)–N(2)	2.680(16)
Pb(1)–N(7)	2.784(17)				
Angle	(°)	Angle	(°)	Angle	(°)
O(1)–Pb(1)–O(3)	85.4(6)	O(1)–Pb(1)–N(2)	76.9(5)	O(3)–Pb(1)–N(2)	73.2(5)
O(1)–Pb(1)–N(7)	71.3(5)	O(3)–Pb(1)–N(7)	85.7(6)	N(2)–Pb(1)–N(7)	143.0(5)

3 RESULTS AND DISCUSSION

3. 1 Structural description

X-ray diffraction study indicates that **1** belongs to the triclinic space group $P\bar{1}$ and the asymmetric unit contains one four-coordinated Pb(II) center, one adipate anion and one L ligand, as shown in Fig. 1. Each Pb(II) enter exhibits a slightly distorted tetrahedral coordinated environment completed by two nitrogen atoms from two symmetry-related L ligands and two oxygen atoms from adipate group. The distances of Pb–O are in the range of 2.448(14)~2.535(17) Å, and Pb(1)–N bond lengths are from 2.680(16) to 2.784(17) Å. The bond angles around the Pb(II) cation are in the range of 71.3(5)~143.0(5)°, all of which fall in the normal range of those observed in the reported Pb(II) complexes[22, 23].

In complex **1**, adipic acids are fully deprotonated, as proved to be no stretching vibration around 1700 cm^{-1} and serves as a monodentate ligand through one carboxylate oxygen atom coordinating to Pb(II). It bridges two adjacent Pb(II) forming a 1D chain (Fig. 2). The Pb(II)–Pb(II) separation across adip is 10.955 and 10.649 Å, respectively. The structure is different with the reported Pb(II) complex, which is a double-line structure because of different carboxylates[24]. Meanwhile, each L ligand also adopts a monodentate coordination mode, and it sits up and down the chain. Additionally, there are C–H···N and C–H···O hydrogen

bonds derived from the pyridine, benzene, imidazloe of L and carboxylic groups of adip^{2-} ligand. The hydrogen-bonding parameters of **1** are listed in Table 2. Moreover, π-π interactions exist between the imidazole ring and the pyridine ring, the imidazole ring and the benzene ring of L ligand, as listed in Table 3. As a result, the complex extends into a three-dimensional supramolecule (Fig. 3) through hydrogen bonds and π-π stacking interactions, so that it is more stable.

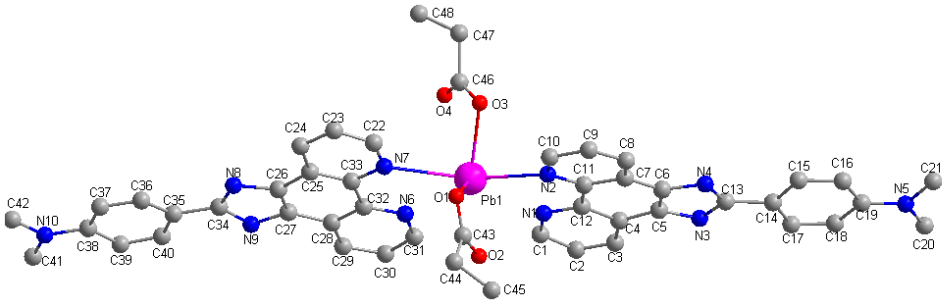

Fig. 1. Coordination environment of Pb(II) ion in 1

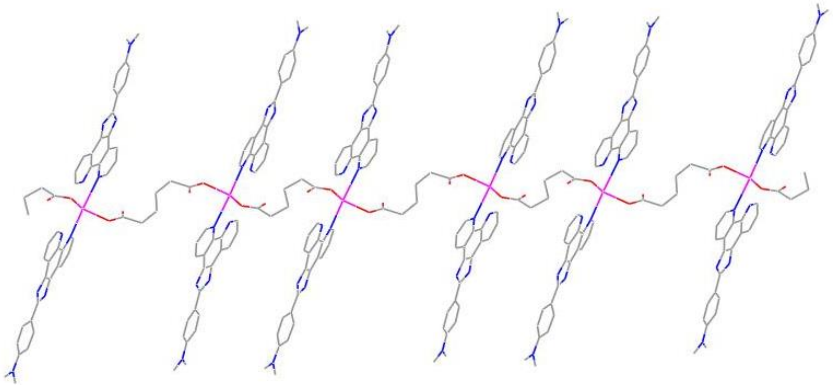

Fig. 2. View of the one-dimensional chain

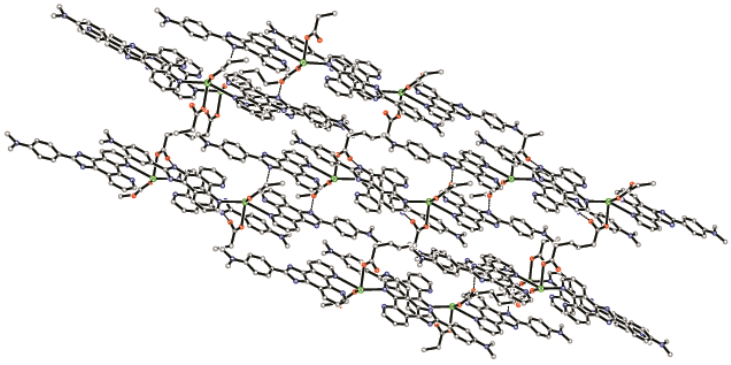

Fig. 3. View of the 3D supramolecular structure of complex 1

Table 2. Hydrogen Bonds for Complex 1

D–H ··A	d(D–H)	d(H ··A)	d(D ··A)	∠(DHA)	Symmetry codes
C(3)–H(3A) ··O(2)	0.93	2.59	3.42(3)	149	1–*x*, 1–*y*, 1–*z*
C(17)–H(17A) ··N(3)	0.93	2.60	2.90(3)	100	
C(17)–H(17A) ··O(2)	0.93	2.46	3.34(3)	160	1–*x*, 1–*y*, 1–*z*
C(40)–H(40A) ··N(9)	0.93	2.58	2.92(3)	102	
C(40)–H(40A) ··O(4)	0.93	2.32	3.23(3)	165	1–*x*, 1–*y*, –*z*

Table 3. Parameters between the Planes in 1

Plane	Distance between ring centroids (Å)	Dihedral angle (°)	Perpendicular distance of plane (I) on ring J (Å)	Perpendicular distance of plane (J) on ring I (Å)
N(8)C(26)C(27)N(9)C(34)–>N(6)C(31)C(30)C(29)C(28) C(32)[2667]	3.880(13)	1	–3.422(9)	–3.396(9)
N(1)C(1)C(2)C(3)C(4)C(12)–>N(1′)C(1′)C(2′)C(3′)C(4′) C(12′)[2668]	3.615(11)	0	3.302(8)	3.302(8)
N(1)C(1)C(2)C(3)C(4)C(12)–>C(4)C(5)C(6)C(7)C(11) C(12)[2668]	3.569(11)	3	3.336(8)	3.287(8)
N(1)C(1)C(2)C(3)C(4)C(12)–>C(35)C(36)C(37)C(38) C(39)C(40)[2667]	3.632(12)	5	–3.592(8)	–3.536(9)
N(6)C(31)C(30)C(29)C(28)C(32)–>C(14)C(15)C(16) C(19)C(18)C(17)[2668]	3.627(13)	6	3.545(9)	3.556(9)
N(6)C(31)C(30)C(29)C(28)C(32)–>C(25)C(26)C(27) C(28)C(32)C(33)[2667]	3.511(12)	0	–3.414(9)	–3.410(9)

[2667] = 1–*x*, 1–*y*, 2–*z*; [2668] = 1–*x*, 1–*y*, 3–*z*

3. 2 IR analysis

IR spectra of **1** with the frequency range of 400～4000 cm^{-1} are shown in Fig. S1. The absorption observed at 3150 cm^{-1} in **1** can be attributed to the ν_{N-H} stretching band of L ligand[25]. The weak absorption peaks of the -CH_3 group of L in **1** is observed at 2918 cm^{-1}[26]. The peaks observed at 1602 cm^{-1} for the complex is assigned to the stretching bands of $\nu_{as(COO-)}$, whereas those at about 1390 cm^{-1} to the stretching bands of $\nu_{s(COO-)}$. The skeletal vibrations of phenyl and pyridyl rings vary from 1587 to 1471 cm^{-1}. The strong bands in the range of 686~735 cm^{-1} can be attributed to the $\nu_{(C-N)}$ stretching of the N-heterocyclic rings of the L ligand[27-29].

3. 3 Powder X-ray diffraction (PXRD) and thermal stability analyses

To confirm that the crystal structures are truly representative of the bulk materials, PXRD experiment was carried out for **1**. As shown in Fig. 4, the experimental powder X-ray diffraction (PXRD) measured and simulated patterns of complex **1** show that the synthesized bulk material is the same as single crystal[30-33]. In order to characterize the thermal stability of **1**, its thermal decomposition behavior was investigated at 30~800 ℃ under N_2 atmosphere using the thermal gravimetric analysis technique. As illustrated in Fig. S2, the weight loss appears in the range of 400~610 ℃ with a very significant loss, which may be corresponding to the decomposition of L ligands and adipate anions. Finally, a yellow residue of PbO (observed 21.16%, calculated 21.71%) is remained. TG result indicates that complex **1** possesses great thermal stability.

3. 4 Photoluminescent properties

The fluorescence properties of the L ligand and the solid phase of complex **1** were determined at room temperature (Fig. 5). The ligand of L has a relatively wide emission peak at 476 nm, upon excitation at 320 nm. And complex **1** also has a relatively wide emission peak at 514 nm, which is upon excitation at 320 nm, too. There is a red shift relative to the emission peak of the L ligand, which is caused by the inductive effect in the structure of L ligand.

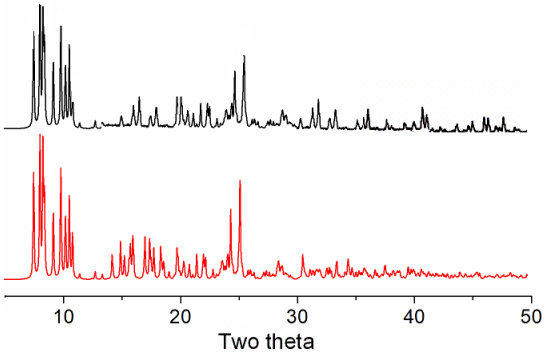

Fig. 4. PXRD analysis of 1: bottom-simulated, top-experimental

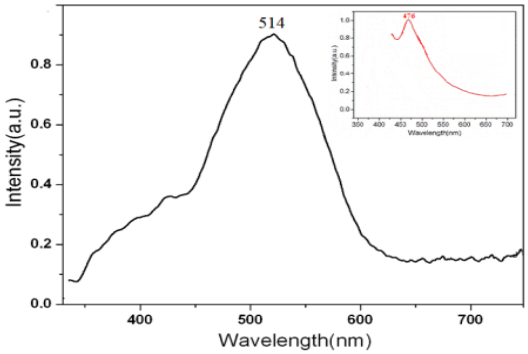

Fig. 5. Solid-state emission spectrum of 1 and L at room temperature

4 QUANTUM CHEMISTRY CALCULATIONS

Quantum chemistry calculations in this manuscript were carried out with the Gaussian16 program[34]. The parameters of the molecular structure for calculation were all from the experimental data of the complex. Natural bond orbital (NBO) study was performed by density functional theory (DFT)[35] with the PBE0[36, 37] hybrid functional and the LANL2DZ basis set[38-40].

The selected natural atomic charges, natural electron configuration, Wiberg bond indices and NBO bond orders (a.u) for **1** are listed in Table 5 with the electronic configurations of Pb(II) ion, nitrogen, and oxygen atoms being $6s^{1.95}6p^{0.63}$, $2s^{1.34\sim1.36}2p^{4.08\sim4.13}$ and $2s^{1.70}2p^{5.06\sim5.007}$, respectively. We infer that the Pb(II) ion coordination with N and O atoms is mainly on 6*s* and 6*p* orbitals. Both N and O atoms form coordination bonds with Pb(II) ion using 2*s* and 2*p* orbitals and Pb(II) ion obtained some electrons from two N atoms of different L ligands and two O atoms of two $adip^{2-}$ ligands[39, 40]. Thus, according to valence-bond theory, the atomic net charge distribution and the NBO bond orders of complex **1** (See Table 4) show obvious covalent interaction between the coordinated atoms and Pb(II) ion. The differences of the NBO bond orders for Pb–O and Pb–N make their bond lengths different[40], which is in good agreement with the X-ray crystal structural data of **1**.

Table 4. Selected Atom Net Charges, Electron Configurations, Wiberg Bond Indexes and NBO Bond Orders of 1

Atom	Net charge	Electron configuration	Bond	Wiberg bond index	NBO bond order
Pb(1)	1.40207	[core]6*s*(1.95)6*p*(0.63)			
O(1)	–0.78686	[core]2*s*(1.70)2*p*(5.07)	Pb(1)–O(1)	0.1845	0.1552
O(3)	–0.77665	[core]2*s*(1.70)2*p*(5.06)	Pb(1)–O(3)	0.1810	0.1489
N(2)	–0.48896	[core]2*s*(1.34)2*p*(4.13)	Pb(1)–N(2)	0.1075	0.1404
N(7)	–0.46150	[core]2*s*(1.36)2*p*(4.08)	Pb(1)–N(7)	0.1038	0.1356

As can be seen from Fig. 6, the lowest unoccupied molecular orbital (LUMO) and the highest occupied molecular orbital (HOMO) are mainly composed of L ligands. Thereby, ILCT may be inferred from some contours of the molecular orbital of **1**.

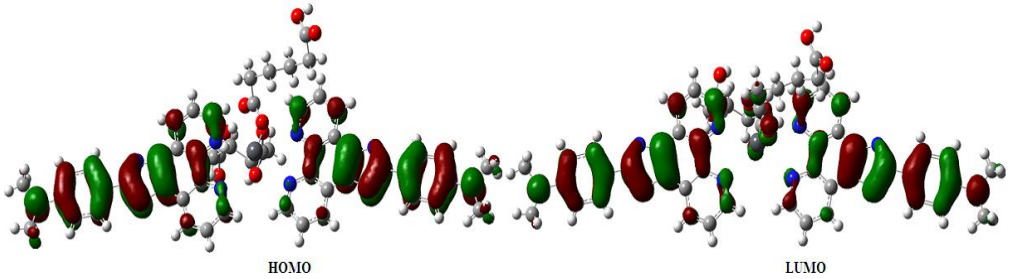

Fig. 6. Frontier molecular orbitals of 1

REFERENCES

(1) Yang, J.; Ma, J. F.; Liu, Y. Y.; Ma, J. C.; Batten, S. R. Organic-acid effect on the structures of a series of lead(II) complexes. *Inorg. Chem.* **2007**, 46, 6542–6555.

(2) Yang, J.; Ma, J. F.; Liu, Y. Y.; Ma, J. C.; Batten, S. R. A series of lead(II) complexes with π-π stackings: structural diversities by varying the ligands. *Cryst. Growth Des.* **2009**, 9, 1894–1911.

(3) Wang, X. L.; Chen, Y.; Gao, Q. Q.; Lin, H. Y.; Liu, G. C.; Zhang, J. X.; Tian, A. X. Coordination behavior of 5,6-substituted 1,10-phenanthroline derivatives and structural diversities by coligands in the construction of lead(II) complexes. *Cryst. Growth Des*. **2010**, 10, 2174–2184.

(4) Wang, X. Y.; Guo, J.; Wang, H. L.; Wang, Q. W. Z. Synthesis and crystal structure of a new Pb(II) coordination polymer constructed by a 1,10-phenanthroline derivative and a flexible dicarboxylate. *Z. Naturforsch*. **2011**, 66b, 647–650.

(5) Wang, X. L.; Gao, Q.; Chen, Y. Q.; Liu, G. C.; Tian, A. X.; Kang, Z. H. Effect of the length of fatty acid ligands on lead(II) complexes based on a 1,10-phenanthroline derivative. *Z. Anorg. Allg. Chem.* **2011**, 637, 142–147.

(6) Cui, L. S.; Meng, X. M.; Li, Y. G.; Huang, K. R.; Li, Y. C.; Long, J. Q.; Yao, P. F. Syntheses, structural diversity, and photocatalytic-degradation properties for methylene blue of Co(II) and Ni(II) MOFs based on terephthalic acid and different imidazole bridging ligands. *CrystEngComm*. **2019**, 21, 3798–3809.

(7) Yang, D. D.; Liu, Y.; Li, S. S.; Cheng, L.; Wang, Y.; Zhang, Y. X.; Chen, K.; Gao, Y. X.; Ren, P.; Day, G. S.; Wang, Y. Ligand-rearrangement-induced transformation from a 3D supramolecular network to a discrete octanuclear cluster: a good detector for Pb^{2+} and $Cr_2O_7^{2-}$. *ACS Omega* **2019**, 4, 11493−11499.

(8) Qian, J.; Sun, M. M.; Liu, M.; Gu, W. Macromolecular probe based on a Ni^{II}/Tb^{III} coordination polymer for sensitive recognition of human serum albumin (HSA) and MnO_4^-. *ACS Omega*. **2019**, 4, 11949−11959.

(9) Wang, J.; Gao, L. L.; Zhang, J.; Zhao, L.; Wang, X. Q.; Niu, X. Y.; Fan, L. M.; Hu, T. P. Syntheses, gas adsorption, and sensing properties of solvent-controlled Zn(II) pseudo-supramolecular isomers and Pb(II) supramolecular isomers. *Cryst. Growth Des*. **2019**, 2, 630−637.

(10) Gao, Q.; Xu, J.; Cao, D. P.; Chang, Z.; Bu, X. H. A rigid nested metal-organic framework featuring a thermoresponsive gating effect dominated by counterions. *Angew. Chem., Int. Ed*. **2016**, 55, 15027−15030.

(11) Zhang, J. W.; Man, Y.; Liu, W. H.; Liu, B. Q.; Dong, Y. P. A Dy_2 dimer derived from a two-dimensional network with a high U_{eff} value. *Dalton Trans.* **2019**, 48, 2560−2563.

(12) Kirchon, A.; Feng, L.; Drake, H. F.; Joseph, E. A.; Zhou, H. C. From fundamentals to applications: a toolbox for robust and multifunctional MOF materials. *Chem. Soc. Rev*. **2018**, 23, 8611−8638.

(13) Fang, W. H.; Yang, G. Y. Induced aggregation and synergistic coordination strategy in cluster organic architectures. *Acc. Chem. Res*. **2018**, 11, 2888−2896.

(14) Li, X. M.; Pan, Y. R.; Zhan, P. Y.; Wang, Q. W.; Liu, B. A new Cd(II) coordination polymer constructed by 3-(2-pyridyl)pyrazole and 5-nitroisophthalic acid: synthesis, crystal structure and theoretical calculations. *Chin. J. Struct. Chem*. **2017**, 36, 1609–1616.

(15) Wang, X. Y.; Li, X. M.; Pan, Y. R.; Liu, B.; Zhou, S. A new three-dimensional Cd(II) complex assembled by 1,3,5-benzenetricarboxylic acid and 3-(2-pyridyl)pyrazole. *Chin. J. Struct. Chem*. **2019**, 38, 1275–1282.

(16) Yang, J.; Ma, J. F.; Liu, Y. Y.; Ma, J. C.; Batten, S. R. A series of lead(II) complexes with π-π stackings: structural diversities by varying the ligands. *Cryst. Growth Des.* **2009**, 9, 1894–1911.

(17) Huang, Y. J.; Ni, L.; Du, G.; Cui, Y. C.; Zhang, W. L.; Wang, L.; Hao, X. R. Synthesis, characterization and crystal structure of two metal-organic complex with MOPIP. *Chin. J. Inorg. Chem*. **2010**, 26, 1269–1273.

(18) Zhao, L. N.; Chen, L.; Liu, B.; Li, X. M.; Wang, Q. W. Hydrothermal synthesis and crystal structure of two three-dimensional supramolecular lead(II) coordination polymers. *Chin. J. Inorg. Chem*. **2013**, 29, 1243–1248.

(19) Liu, B.; Zhou, S.; Li, X. M.; Li, C. B. A new chain-like copper(Ⅱ) polymer: $[Cu(MOPIP)(BDC)]_n$ 0.5n(H_2O). *Chin. J. Struct. Chem*. **2008**, 27, 1195–1198.

(20) Sheldrick, G. M. *SHELXS 97, Program for the Solution of Crystal Structure*. University of Göttingen, Germany **1997**.

(21) Sheldrick, G. M. *SHELXL 97, Program for the Refinement of Crystal Structure*. University of Göttingen, Germany **1997**.

(22) Li, Y.; Zou, X. Z.; Qiu, W. D.; Feng, A. S.; Chen, X. L. Syntheses, crystal structures, magnetic and luminescent properties of Ni(II), Cd(II) and Pb(II) coordination compounds constructed from 5-fluoronicotinic acid. *Chin. J. Struct. Chem*. **2019**, 38, 999–1011.

(23) Chen, L.; Wang, Y. L.; Liu, Q. Y.; Yao, Y. Solvothermal synthesis, crystal structure and luminescent property of a two-dimensional lead(II) compound:

[Pb(bmzbc)$_2$]$_n$. *Chin. J. Struct. Chem*. **2016**, 35, 615–620.

(24) Liu, G. C.; Guo, Z. C.; Wang, X. L.; Qu, Y.; Yang, S.; Lin, H. Y. Tuning 1-D Pb(II) coordination polymers by flexible and semirigid dicarboxylates: synthesis, structure and properties. *Z. Naturforsch*. **2012**, 67b, 18–191.

(25) Bellamy, L. J. *The Infrared Spectra of Complex Molecules.* Wiley: NY **1958**.

(26) Gu, X. J.; Xue, D. F. Selected controlled synthesis of three-dimensional 4*d*-4*f* heterometallic coordination frameworks by lanthanide carboxylate subunits and silver centers. *Cryst. Growth Des*. **2006**, 6, 2551–2557.

(27) Uddin, M. N.; Ferdous, T.; Islam, Z.; Jahan, M. S.; Quaiyyum, M. A. Development of chemometric model for characterization of non-wood by FT-NIR data. *J. Bioresour. Bioprod*. **2020**, 5, 196–203.

(28) Chen, Z. J.; Gao, H.; Li, W.; Li, S. J.; Liu, S. X.; Li, J. Research progress of biomass-based optical materials. *J. For. Eng.* **2020**, 5, 1−12.

(29) Zhang, J. Y.; Lei, H. J.; Zhou, S. P.; Li, S. J.; Deng, Z. H.; Shi, Z. J. Synthesis of TiO_2/walnut shell carbon photocatalyst and its activity for phenol degradation. *J. For. Eng.* **2020**, 5, 104−108

(30) Yorseng, K.; Siengchin, S.; Ashok, B.; Rajulu, A. V. Nanocomposite egg shell powder with in situ generated silver nanoparticles using inherent collagen as reducing agent. *J. Bioresour. Bioprod*. **2020**, 5, 101−107.

(31) Ashok, B.; Hariram, N.; Siengchin, S.; VaradaRajulu, A. Modification of tamarind fruit shell powder with in situ generated copper nanoparticles by single step hydrothermal method. *J. Bioresour. Bioprod*. **2020**, 5, 180−185.

(32) Cai, Z. Y.; Zhu, H. X.; Wang, P.; Wu, C. Y.; Gao, W. C.; Mu, J. Y.; Wei, S. Y. Performance optimization of UV curable waterborne polyurethane acrylate wood coatings modified by castor oil. *J. For. Eng.* **2020**, 5, 89−95.

(33) Kan, Z. Y.; Kan, H. F.; Jiang, Y.; Ge, J.; Zhu, M. Q.; Wu, D.; Gao, Z. H. Optimal synthesis of urea-glyoxal resin and its crosslinking modification on soybean-based wood adhesive. *J. For. Eng.* **2020**, 5, 69−75.

(34) Frisch, M. J.; Trucks, G. W.; Schlegel, H. B.; Scuseria, G. E.; Robb, M. A. *Gaussian 03*, Revision B.16; Gaussian, Inc., Pittsburgh, PA **2016**.

(35) Parr, R. G.; Yang, W. *Density Functional Theory of Atoms and Molecules*. Oxford University Press: Oxford **1989**.

(36) Ernzerhof, M.; Scuseria, G. E. Assessment of the Perdew-Burke-Ernzerhof exchange-correlation functional. *J. Chem. Phys*. **1999**, 110, 5029–5036.

(37) Adamo, C.; Barone, V. Toward reliable density functional methods without adjustable parameters: the PBE0 model. *J. Chem. Phys*. **1999**, 110, 6158–6170.

(38) Dunning, T. H. Jr.; Hay, P. J. *In Modern Theoretical Chemistry*. Schaefer HF, III, Ed.; Plenum: New York **1976**, 3, 1–28.

(39) Wang, L.; Zhao, J.; Ni, L.; Yao, J. Synthesis, structure, fluorescence properties, and natural bond orbital (NBO) analysis of two metal [Eu^{III}, Co^{II}] coordination polymers containing 1,3-benzenedicarboxylate and 2-(4-methoxyphenyl)-1H-imidazo[4,5-f][1,10-] phenanthroline ligands. *ZAAC* **2012**, 638, 224–230.

(40) Li, Z. P.; Xing, Y. H.; Zhang, Y. H. Synthesis, structure and quantum chemistry calculation of scorpionate oxovanadium complexes with benzoate. *Acta Phys. Chim. Sin*. **2009**, 25, 741–746.